Light Scattering Studies of Poly(dimethylsiloxane) Solutions and Swollen Networks

V. K. Soni*,† and R. S. Stein

Polymer Research Institute, University of Massachusetts, Amherst, Massachusetts 01002

Received December 1, 1989; Revised Manuscript Received May 15, 1990

ABSTRACT: Static light scattering measurements were performed on model poly(dimethylsiloxane) (PDMS) networks swollen to equilibrium in toluene and in benzene. In comparison to solutions of linear chains of equal polymer concentration, the swollen networks scatter more light. This excess scattering of light has been analyzed in terms of concentration fluctuations due to variations in the local cross-link density. Bimodal networks of controlled distributions of molecular weights between cross-links were used to study the effects of cross-link inhomogeneities. The experimental results are compared to theoretical estimates based upon the macroscopic composition of the network. The observed discrepancy suggests the necessity for an improvement in the description of the microscopic or local swelling behavior in networks.

I. Introduction

The scattering of light by inhomogeneously cross-linked polymer networks was described many years ago by one of us.[1] Another approach to this problem and some preliminary experimental data were reported by Bueche.[2] In this paper, we report the results of some measurements on swollen, model poly(dimethylsiloxane) (PDMS) networks that disagree with the simple theories. These point the way to an improved theoretical description, preliminary aspects of which are described.

The scattering of light by inhomogeneous, isotropic systems arises from fluctuations in refractive index and has been described in a statistical theory by Debye and Bueche.[3] In order to describe the scattering from swollen networks, it is necessary to relate the scattered intensity to the equilibrium properties of a network. Although the molecular basis for rubberlike elasticity is well understood,[4] there is considerable disagreement regarding the role of the network structure or topology.

Using model networks, Mark and co-workers[5-7] have shown that the stress–strain and swelling behavior of unimodal networks can be described reasonably well by the Flory–Erman theory.[8] They have prepared bimodal PDMS networks using known amounts of short and long chains.[9] Some of these networks, typically 90 mol % of short chains, have remarkably high ultimate mechanical properties, i.e., high moduli at large extension ratios.

The light scattering experiments presented in this paper were originally planned for characterization of the distribution of molecular weights between cross-links. The initial analysis was made utilizing the assumption that macroscopic scattering theories could be applied at a microscopic level in an inhomogenous network. This did not work but, as will be shown in the following sections, the study of light scattering from such swollen inhomogenous networks offers a new approach to test rubber elasticity theory.

A. Scattering from Inhomogeneous Systems. The scattering power of a material is usually defined in terms of the Rayleigh ratio of an isolated infinitesimal element of volume u

$$R(q) = I(q)p^2/I(0)u \tag{1}$$

where p is the sample-to-detector distance and $I(q)$ is the scattered intensity at a reduced scattering angle, q, defined as

$$q = (4\pi/\lambda)\sin(\theta/2) \tag{2}$$

where λ is the wavelength of the radiation in the medium and θ is the angle between the incident and scattered ray measured in the scattering medium.

The scattering from an isotropic medium having fluctuations in refractive index is described by the Debye–Bueche[3] theory as

$$R(q) = 4\pi K\langle\eta^2\rangle\int\frac{\gamma(r)\sin(qr)r^2}{qr}\mathrm{d}r \tag{3}$$

$\langle\eta^2\rangle$ is the mean squared fluctuation in the refractive index, $\gamma(r)$ is a spatial correlation function defined as

$$\gamma(r) = \langle\eta_i\eta_j\rangle_r/\langle\eta^2\rangle \tag{4}$$

where η_i and η_j are the fluctuations in the refractive index at positions i and j separated by a distance r, and $\langle\ \rangle_r$ represents the average overall pairs of scattering elements with a constant separation of r. This function describes the geometry of the fluctuation and decreases from unity at $r = 0$ toward zero at $r = \infty$ in a manner dependent on the size of the region over which the fluctuation occurs. In eq 3, K is a constant equal to $4\pi^2n^2/\lambda_0^4$, where λ_0 is the wavelength of the radiation in a vacuum and n is the refractive index of the medium.

It has been shown that for many systems,[3] $\gamma(r)$ may be adequately represented by an exponential function

$$\gamma(q) = \exp(-r/a_c) \tag{5}$$

where a_c is a parameter measuring the size of the correlated regions called the correlation length. For such a correlation function eq 3 becomes

$$R(q) = \frac{8\pi K a_c^3\langle\eta^2\rangle}{(1 + q^2a_c^2)^2} \tag{6}$$

Thus, a plot of $R(q)^{-0.5}$ versus q^2 should provide a straight line. From the intercept of such a Debye–Bueche plot, $\langle\eta^2\rangle$ can be estimated and from the slope, a_c can be calculated.

B. Scattering from Polymer Solutions. In the case of scattering of light for a vertically polarized incident beam, if the analyzer is horizontal, the scattering geometry will be referred to as H_v, and scattering occurs as a consequence of the anisotropy in the material. For V_v geometry, the analyzer is vertical, and the scattering

† Present address: Polaroid Corp., 750 Main Street, 5C, Cambridge, MA 02139.

0024-9297/90/2223-5257$02.50/0

contains contributions arising from both isotropic and anisotropic polarizability fluctuations.

The isotropic scattering for a system possessing some anisotropic polarizability fluctuations can be obtained as[10]

$$R_{iso} = R_{V_v} - 4R_{H_v}/3 \tag{7}$$

At low polymer concentrations, the scattered intensity from polymer solutions can be considered as the sum of scattering due to density and concentration fluctuations

$$R_{iso} = R_c + R_d \tag{8}$$

The scattering due to density fluctuations can be expressed as[11]

$$R_d = \frac{\pi^2 kT\beta}{\lambda_0^4}[\rho(\partial\epsilon/\partial\rho)_T]^2 \tag{9}$$

where β is the bulk isothermal compressibility, k is Boltzmann's constant, ρ is the density, and ϵ is the optical dielectric constant. The Eykman expression[10,13] can be used for $[\rho(\partial\epsilon/\partial\rho)_T]$

$$\rho(\partial\epsilon/\partial\rho)_T = \frac{2n(n+0.4)(n^2-1)}{n^2+0.8n+1} \tag{10}$$

where n is refractive index. The concentration fluctuation term in eq 8 is given by

$$R_c = K_L kTc/(\partial\Pi/\partial c)_T \tag{11}$$

where c is the polymer concentration, Π is the osmotic pressure, and K_L is the light scattering constant, which is given by

$$K_L = \frac{4\pi^2 n^2(\partial n/\partial c)^2}{\lambda_0^4} \tag{12}$$

where $(\partial n/\partial c)$ is the refractive index increment.

At moderate concentrations, density and concentration fluctuations are interdependent. To account for such an interdependence, Bullough[12,13] has proposed an amended form of eq 8

$$R_c = R_{iso} - R_d(1+4Y) \tag{13}$$

where

$$Y = \frac{cn(\partial n/\partial c)_T}{\rho(\partial\epsilon/\partial c)_T} \tag{14}$$

For concentrated solutions, one can use the Flory–Huggins equation[14] for osmotic pressure

$$\Pi = \frac{-kT}{V_1}[\ln(1-v_2) + (1-x_w^{-1})v_2 + \chi v_2^2] \tag{15}$$

where v_2 is the volume fraction of polymer ($c = v_2\rho_2$). x_w is the weight-average degree of polymerization for the polymer, χ is the polymer–solvent interaction parameter, and V_1 is the partial molar volume of the solvent.

Using eq 15 in eq 11, we have

$$R_c = \frac{K_L V_1 v_2 \rho_2^2}{(1-v_2)^{-1} + (x_w)^{-1} - 1 - 2\chi v_2} \tag{16}$$

Such an expression can account for a maximum in R_c as a function of concentration as was observed by Debye and Bueche.[15] The position of the maxima depends on the size of the polymer chain, moving to lower concentrations for longer chain lengths.

In eq 15, χ has been assumed to be independent of concentration. However, one can consider a concentration-dependent $\chi = \chi_0 + \chi_1 v_2$, which leads to an additional term in the denominator of eq 16.

C. Scattering from Swollen Networks. For a network swollen at equilibrium, the osmotic pressure can be expressed in terms of the Flory–Rehner theory[14] as

$$\Pi = \frac{-kT}{V_1}\left[\ln(1-v_2) + v_2 + \chi v_2^2 + \frac{(\rho_2 V_1)}{M_c}[v_2^{1/3} - v_2/2]\right] \tag{17}$$

where M_c is the molecular weight between cross-links. Therefore, for an ideal network the expression for R_c can be obtained by using eq 17 in eq 11, giving

$$(R_c)_{ideal} = \frac{K_L V_1 \rho_2^2 v_2}{(1-v_2)^{-1} - 1 - 2\chi v_2 + (\rho_2 V_1/6M_c)(3 - 2v_2^{-2/3})} \tag{18}$$

The intensity of scattering from real swollen networks is usually much greater than that predicted by eq 18. We believe that this excess scattering primarily arises from inhomogeneities in the network.

Inhomogeneously cross-linked networks swell nonuniformly. If there is sufficient difference in the refractive index between the polymer and diluent, then the nonuniform distribution of solvent in the swollen network can be studied by light scattering in order to estimate the inhomogeneity in the cross-link density. This has been the approach proposed by Stein,[1] Bueche,[2] and Wun and Prins.[17]

The local $(M_c)_i$ deviates from the mean M_c as

$$(\Delta M_c)_i = M_c - (M_c)_i$$

The corresponding fluctuation in the local concentration of polymer will be $(\Delta v_2)_i$. Using the Flory–Rehner theory for swelling, Stein[1] showed that

$$(\Delta v_2)_i = Q(v_2)[(\Delta M_c)_i/M_c] \tag{19}$$

where Q is a function of v_2 and χ. For high degrees of swelling $Q = -3v_2/5$. This assumes that the Flory–Rehner theory can be applied at a local level and that, if there is a distribution of molecular weight, the local degree of swelling at the location of a particular chain depends upon the molecular weight of that chain *alone*. The correctness of this assumption will be discussed later.

The total isotropic scattering from swollen networks can be considered as a sum of three terms

$$R_{iso} = (R_c)_{ideal} + R_d(1+4Y) + R_E \tag{20}$$

where R_E represents the excess scattering due to cross-link density inhomogeneities. According to Stein[1]

$$R_E = 4\pi\langle\eta^2\rangle K\int\frac{\gamma(r)\sin(qr)r^2}{qr}dr \tag{21a}$$

where

$$\langle\eta^2\rangle = \frac{(n_1-n_2)^2\langle\Delta M_c^2\rangle Q^2}{M_c^2} \tag{21b}$$

The correlation function $\gamma(r)$ can be defined as

$$\gamma(r) = \frac{\langle(\Delta M_c)_i(\Delta M_c)_j\rangle_r}{\langle\Delta M_c^2\rangle} \tag{21c}$$

The scattered intensity can be measured as a function of the scattering angle. Thus, the correlation size a_c and $\langle\Delta M_c^2\rangle$ can be estimated from the slope and intercept of the Debye–Bueche plot using eq 6.

Table I

sample	η^a	M_n	M_w	M_w/M_n
PDMS-4-6	5	770	1450	1.88
PDMS-1000	1000	22500	40600	1.80

[a] In centistokes.

II. Experimental Section

A. Prepolymers. Model poly(dimethylsiloxane) (PDMS) networks for this study were prepared by end-linking α,ω-divinyl-PDMS with tetrakis(dimethylsiloxy)silane in the presence of a platinum catalyst (PC072).

The two PDMS prepolymers that were usd are listed in Table I. All the reactants were purchased from Petrarch Systems, Bristol, PA. The advantages of using such a PDMS system are as follows:

(i) M_c and functionality in the network can be controlled.

(ii) The prepolymers have a reasonably low viscosity. This makes filtration of the bulk polymer easy.

(iii) The resulting networks have excellent optical clarity, even in thick films.

(iv) The cross-linking reaction proceeds by addition, and therefore no low molecular weight compound has to be removed during the cure.

(v) The cross-linking agent is very similar to the chain repeat units.

The major drawback in using such polymer is the polydispersity $M_w/M_n \sim 1.8$. The details of the analysis of the prepolymers are given elsewhere.[18].

B. Sample Preparation. The general procedures followed for curing the PDMS networks are along the lines of those developed by Mark and co-workers.[5-7] The prepolymers were filtered through a 0.5-μm Millipore filter. The required amount of catalyst solution (0.5 ppm Pt) was added to the prepolymer, and the two were mixed under vacuum for 1 h. The required amount of cross-linker was added under an inert nitrogen atmosphere. The reactants were mixed together for 15–20 min and then poured into the mold. The curing reaction was allowed to proceed for 1 day at room temperature followed by 1 day at 60 °C.

The mold used was made of aluminum and was designed to ensure uniform sample thickness.[18] The top and bottom surfaces of the mold were polished smooth, and Mylar sheets were attached to the mold faces to ensure smooth sample surfaces and for ease of sample removal from the mold. Samples with thicknesses from 1 to 6 mm could be prepared by using different spacers.

The cured networks were extracted in benzene for 5–6 days to remove the sol fraction. The sol fraction was found to be ca. 3–4%. Meyers et al.[19] have observed that cyclics account for a large fraction of the sol extracted from such networks. After extraction of the sol, the samples were deswollen and then swollen in fresh benzene and toluene for equilibrium swelling measurements.

C. Refractive Index Measurements. An Abbe refractometer (American Optical Model 10450) was used to measure the refractive indices of PDMS solutions in benzene and in toluene. The measurements were made at 25 °C, and the wavelength of the light source was 5890 Å.

D. Light Scattering. The light scattering experiments of PDMS solutions and swollen networks were performed in Professor K. Langley's laboratory at the University of Massachusetts, Amherst. The light source used was a Spectra Physics 165 argon ion laser with a wavelength of 5145 Å. The beam passes through a polarizer, a beam monitor, a focusing lens, the sample chamber, and an analyzer before entering the detector. The detector is a photon counter that is connected to a Langley-Ford digital correlator. The detector arm contains two slits that help control the scattering volume and stray light. The accessible nominal scattering angles are from 30° to 135°.

The samples were held in a thermostatic glass vat that contained an excess of solvent to minimize stray light. Pyrex test tubes with an inner diameter of 10 mm were used as sample cells for solutions and the pure components. For the swollen networks, flat rectangular slabs of ca. 6-mm thickness were used as samples. These were held in a black anodized aluminum sample holder

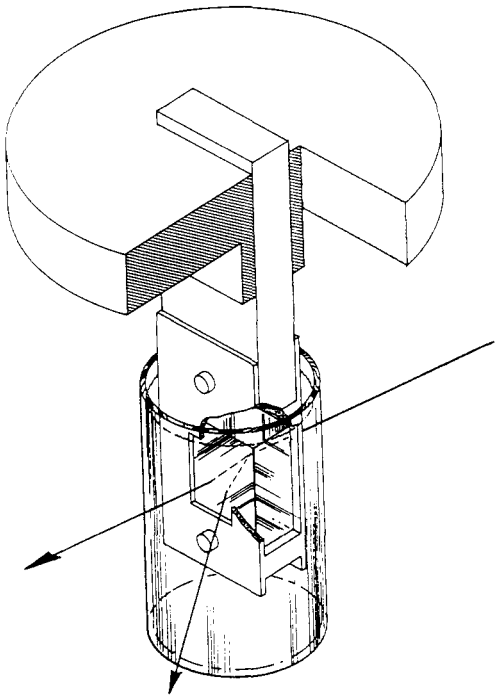

Figure 1. Sketch of sample holder for flat, swollen network samples used in the light scattering experiment. The sectioning allows visualization of the light beam through the sample.

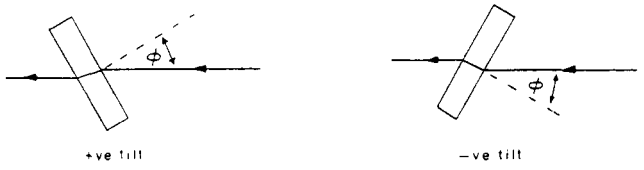

Figure 2. Sketch of the two types of tilt angles used for the flat, swollen network samples.

(Figure 1). The sample holder consists of two parts—a base and a stem. The sample is mounted onto the stem in between two windows. The windows are designed to grip the samples firmly but still provide openings for the incident and scattered beams to pass through. The stem is attached to the base and can be moved up and down so as to expose different parts of the sample to the beam. The base is attached to the frame, which can be rotated to allow different tilt angles (−30°, 0°, and +30°) as shown in Figure 2. The flat samples have to be tilted to allow measurements of scattering at wide angles.

Initially, experiments were tried with cylindrical samples using a special cylindrical holder to suspend the sample into the vat. The main advantage of the cylindrical samples is that the data reduction is simple in that correction for refraction at interfaces is not necessary. The scattering of laser light from the swollen gels results in speckle patterns. The size of the speckles depends on the size of the front slit. The larger the aperture, the smaller the speckle. If the speckle pattern is large, then there are large fluctuations in the intensity. Therefore, it is necessary to average over large scattering volumes to reduce the fluctuations in intensity. To minimize fluctuations associated with the speckle patterns, it was necessary to use the largest possible front aperture and an unfocused beam. When the unfocused beam is incident on a swollen cylindrical gel and solvent, the sample acts as a cylindrical lens and results in the scattered intensity which is independent of angle. Therefore, to minimize the lens effect in using the unfocused beam, it was necessary to use flat samples.

The flat samples were prepred as described in section IIB using a special aluminum mold lined with Mylar sheets to give smooth sample surfaces. Thick samples (~6 mm) were used. A wide range of nominal scattering angle q was covered by using various tilt angles and forward and back scattering geometries. These are shown in Table II. Φ_t is the tilt angle. At each scattering

Table II
Scattering Angles θ Accessible at Various Tilt Angles Φ_t

Φ_t, deg	θ, deg
0	30–50
	120–130
+30	35–80
-30	110–130

Table III
Swelling Results for Bimodal Networks

x	$\langle M_c \rangle$	v_{2B}	F_4	v_{2T}	χ_{Tol}
0	22500	0.200	0.61	0.161	0.51
25	17068	0.230	0.69	0.192	0.52
50	11635	0.276	0.79	0.251	0.547
75	6203	0.330	0.81	0.301	0.554
90	2943	0.380	0.64	0.339	0.550
95	1857	0.439	0.71	0.402	0.563
100	770	0.535	0.68	0.504	0.581

angle, the sample holder was rotated by 180° to expose both faces of the sample and therefore get an average value for the scattered intensity.

For absolute intensity calibration, the total scattering from density fluctuations in toluene was measured at $\theta = 90°$. Kaye and McDaniel[20] have reported that for toluene at 23 °C for $\lambda_0 = 6328$ Å, $R(90°) = 14.06 \times 10^{-6}$ cm^{-1}. Converting to $\lambda_0 = 5145$ Å at 25 °C, one has $R(90°) = 32.85 \times 10^{-6}$ cm^{-1}.

For flat samples, there is concern about specular reflections for the back-scattered light. For a tilt of $\Phi_t = -30°$, one expects a specular reflection at a scattering angle $\theta = 120°$. When the stem in the sample holder is vertical, the specular reflection can be detected at $\theta = 120°$. The narrow width of the specular reflection, in terms of θ, indicated that the surface of the sample is fairly smooth. Specular reflections in the plane of the detector are eliminated by a slight tilt of the sample holder stem in the vertical plane. The corrections necessary for analyzing scattering from tilted thick, flat samples are given in the Appendix. They are based on the analysis developed by Stein and Keane[22] for tilted thin samples.

III. Results

A. Network Swelling. The volume fraction of polymer in the swollen network at equilibrium v_2 can be described by the Flory–Erman theory[8] as

$$M_c = \frac{F_\phi \rho_2 V_1 [(2v_2/\phi) - v_2^{1/3}]}{[\ln(1 - v_2) + v_2 + \chi v_2^2]} \tag{22}$$

where ϕ is the junction functionality and F_ϕ is the front factor in the Flory–Erman theory. In eq 22 χ can be concentration dependent. For PDMS in benzene at room temperature, Mark an co-workers[6] have used

$$\chi = 0.484 + 0.33v_2$$

For unimodal PDMS networks, Mark an co-workers[6] have found that

$$F_4 = 0.65 \pm 0.10$$

In addition to unimodal networks, bimodal networks were also prepared by mixing different mole fractions of short (PDMS-4–6) and long chains (PDMS-1000). If x is the mole fraction of short chains, the average $\langle M_c \rangle$ for a bimodal network will be

$$\langle M_c \rangle = xM_s + (1 - x)M_L \tag{23}$$

M_S and M_L refer to the number-average molecular weights for the short and long chains. The swelling results for the different samples are given in Table III. v_{2B} and v_{2T} refer to the equilibrium swelling volume fractions of polymer in the networks swollen in benzene and toluene, respectively. F_4 was calculated with the PDMS–benzene data. With these values of F_4 for the toluene system, the χ for the PDMS–toluene system, shown as χ_{Tol} in Table III, was estimated. From these data we have

$$\chi_{Tol} = 0.487 + 0.192v_2$$

The values of F_4 in Table III agree reasonably well with the values observed by Mark and co-workers. This suggests that the macroscopic swelling of these bimodal networks is reasonably well described by the Flory–Erman theory.

Table IV
Refractive Indices and Coefficients for the Cauchy Formula (Eq 24) at 25 °C for Different Materials

sample	A	B	n(5145 Å)
toluene	1.4680	8942.8	1.5018
benzene	1.4702	9439.0	1.5058
PDMS-1000	1.3898	4676.9	1.4074

B. Refractive Indices. The Abbe refractometer uses light with a wavelength corresponding to the sodium line ($\lambda = 5890$ Å). Since the light scattering experiments were performed with an argon ion laser ($\lambda = 5145$ Å), it is necessary to estimate n at $\lambda = 5145$ Å. At a given temperature, the wavelength dependence of n can be expressed in terms of the Cauchy dispersion formula[21]

$$n = A + \frac{B}{\lambda_0^2} + \frac{C}{\lambda_0^4} \tag{24}$$

The Cauchy formula is often used in its simplified form with just two terms A and B. Using the Abbe refractometer measurements and values of n reported in the literature[21] at different wavelengths, we estimated A and B for toluene, benzene, and PDMS at 25 °C. These values are given in Table IV along with values of n at $\lambda = 5145$ Å.

For the polymer solutions, the refractive indices at 25 °C and $\lambda_0 = 5145$ Å were estimated by using the Lorenz–Lorentz equation.[21]

$$\frac{[n^2 - 1]}{\rho[n^2 + 2]} = \frac{W_1[n_1^2 - 1]}{\rho_1[n_1^2 + 2]} + \frac{W_2[n_2^2 - 1]}{\rho_2[n_2^2 + 2]} \tag{25}$$

The terms on the left-hand side of eq 25 refer to the solution, and those on the right-hand side refer to the individual pure components. W_i and ρ_i refer to the weight fraction and mass density of the species i. Using the measurements of n at $\lambda_0 = 5890$ Å for the solutions, one can estimate from eq 25 the density of the polymer solution ρ. With these values of ρ and the values of $n_i(\lambda_0 = 5145$ Å) from Table IV, n for the solutions can be estimated.

For PDMS-1000 solutions in toluene and benzene, n was estimated as a function of polymer concentration at 25 °C and $\lambda_0 = 5145$ Å. The results are as follows:

(a) For PDMS-1000 in toluene

$$n = 1.5018 - 0.103v_2 \tag{25a}$$

Since the mass density of PDMS-1000 is almost the same

(b) For PDMS-1000 in benzene

$$n = 1.5058 - 0.112v_2 \tag{25b}$$

as that of the dry (0.97 g/cm^3) networks, the refractive indices for the swollen networks were estimated by using eqs 25a and 25b.

C. Light Scattering from Solutions. The light scattering measurements were made at 25 °C using Pyrex

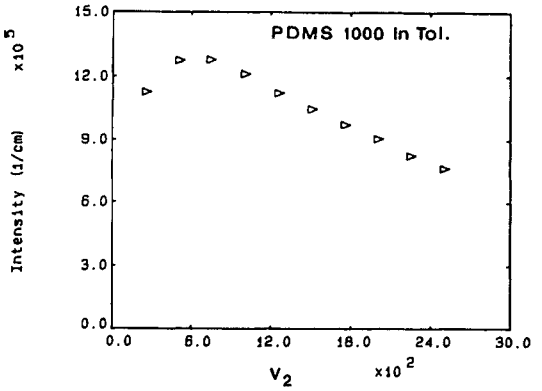

Figure 3. Rayleigh ratio R_{iso} as a function of polymer concentration for PDMS-1000 solutions in toluene at 25 °C.

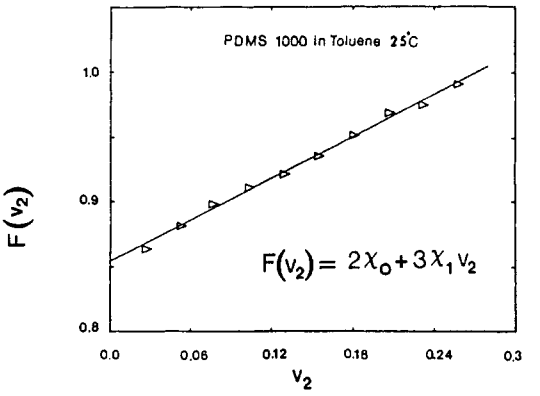

Figure 4. Plot of $F(v_2)$ versus v_2 for PDMS-1000 solutions in toluene at 25 °C.

test tubes as sample holders. The intensity was corrected for dark currents in the beam monitor and the detector and dead time effects in the beam monitor. For all liquid samples measurements were made in the angular range 45–135°. For a cylindrical sample holder, the Rayleigh ratio will be

$$R(\theta) = KI(\theta) \sin \theta \tag{26}$$

where sin θ is the scattering volume correction and K is the instrument constant. For the pure component liquids studied, $R(\theta)$ was found to be independent of θ. The total scattering from toluene at $\theta = 90°$ was used for absolute intensity calibration.

The scattering from the pure components arises due to density fluctuations and can be used to estimate the bulk isothermal compressibility β from eq 9. The results are

$$\beta_{Tol} = 9.6 \times 10^{-11} \text{ cm}^2 \text{ dyn}^{-1}$$

$$\beta_{PDMS} = 12.0 \times 10^{-11} \text{ cm}^2 \text{ dyn}^{-1}$$

These results are in good agreement with values estimated by Huglin and Sokro.[13]

For the solutions the compressibility was approximated as a linear sum

$$\beta = \beta_1 v_1 + \beta_2 v_2 \tag{27}$$

where v_i is the volume fraction of component i.

The Rayleigh ratio for the solutions R_{sol} is given by

$$R_{sol} = \frac{I_{sol} n_{sol}^2 R_{Tol}}{I_{Tol} n_{Tol}^2} \tag{28}$$

where the subscript Tol refers to toluene. The refractive index terms are included to correct for the different solid angles due to refraction.

Figure 3 shows the Rayleigh ratio R_{iso} as a function of polymer concentration for PDMS-1000 solutions in toluene at 25 °C. It can be seen that R_{iso} goes through a maximum as a function of concentration, as was observed by Debye and Bueche.[15] Considering χ to be concentration dependent as $\chi = \chi_0 + \chi_1 v_2$, eq 16 is modified to

$$R_c = \frac{K_L V_1 v_2 \rho_2^2}{(1 - v_2)^{-1} - 1 - x_w^{-1} - 2\chi_0 v_2 - 3\chi_1 v_2^2} \tag{29}$$

Equation 29 can be rearranged to

$$F(v_2) = v_2^{-1}\left[(1 - v_2)^{-1} - 1 - x_w^{-1} - \frac{K_L V_1 v_2 \rho_2^2}{R_c}\right] = 2\chi_0 + 3\chi_1 v_2 \tag{30}$$

Therefore from a plot of $F(v_2)$ vs v_2, χ can be estimated.

Figure 4 shows such a plot. For PDMS-1000 at 25 °C in toluene

$$\chi = 0.43 + 0.1794 v_2$$

From swelling of PDMS networks in toluene we had estimated

$$\chi = 0.487 + 0.192 v_2$$

Assuming a 3% error in the swelling measurements, we expect the standard deviation in the value of χ to be 15%. Therefore, within experimental error, the two expressions of χ are in good agreement.

D. Light Scattering from Swollen Networks. To obtain $R(\theta)$ for flat, tilted samples it is necessary to correct for tilt and refraction. Stein and Keane[22] have reported all the necessary corrections for light scattering from flat, tilted thin films. Their analysis has been modified here for the case of thick samples. $R(\theta)$ is then expressed in terms of the measured intensity $I(\theta)$ and the various correction factors as

$$R(\theta) = \frac{KI(\theta) C_n Z}{I_0 V_s} \tag{31}$$

where C_n is the refraction correction for the solid angle, Z is the correction for reflection, I_0 is the incident intensity, V_s is the scattering volume correction for tilt and refraction, and K is the instrument constant, which includes the size of the apertures, the width of the incident beam, transmission of the attenuators and the analyzer, etc. The ratio K/I_0 can be used as the absolute intensity calibration factor by measuring the scattering from the swollen samples with the same apertures, attenuation, and beam monitor settings as for scattering from toluene. Detailed expressions for the various correction factors listed in eq 31 are given in the Appendix.

For the bimodal networks swollen in toluene and in benzene, the isotropic scattering intensity R_{iso} was estimated by using eq 7. The H_v scattering in the swollen networks is found to be on the order of a few percent of the V_v scattering. Figure 5 shows the measusred V_v and H_v intensities at various nominal scattering angles for a PDMS-1000 network (100% long chains) swollen in toluene. H_v scattering is caused by orientation fluctuations. In the case of swollen networks such fluctuations are possibly due to strains in the sample due to swelling. Considerable H_v scattering can result if the samples are cut in the swollen state. The least amount of H_v scattering was obtained when the samples were cut in the dry state and allowed to swell in the diluent for at least a week.

The contribution of density fluctuations to the isotropic scattering was estimated by using eqs 9 and 13. Equation

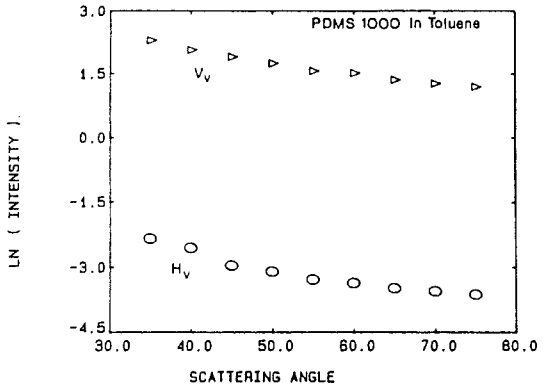

Figure 5. Raw V_v and H_v light scattering data for PDMS-1000 network swollen in toluene.

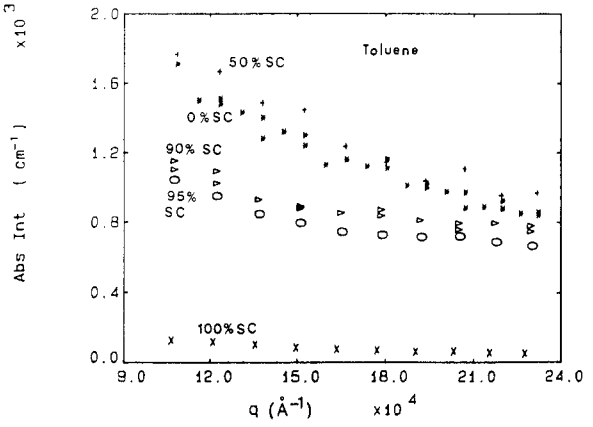

Figure 6. Corrected, absolute intensity light scattering data for bimodal PDMS networks in toluene.

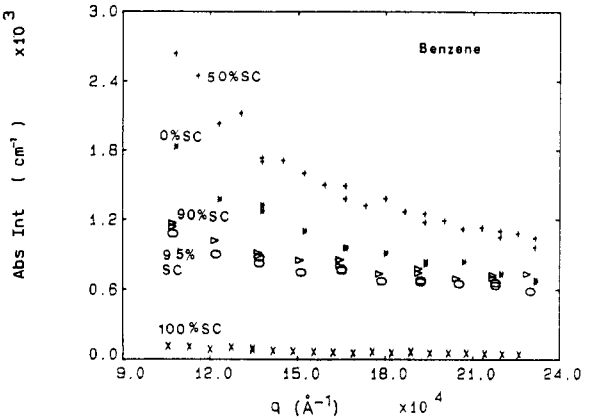

Figure 7. Corrected, absolute intensity light scattering data for bimodal PDMS networks in benzene.

18 was used to estimate the isotropic scattering due to concentration fluctuations in an ideal network having the same degree of swelling and the same average cross-link density as the network being studied. Then the excess scattered intensity or Rayleigh ratio was calculated from eq 20. Figures 6 and 7 show the angular dependence of the excess scattering data $R_E(q)$ vs q for different bimodal PDMS networks swollen in toluene and in benzene. Figures 8 and 9 show the Debye–Bueche plots, eq 6, for the excess scattering from two swollen PDMS networks. From the slope and intercept of the Debye–Bueche plots one can estimate the correlation size a_c and mean squared scattering power.

If the excess scattering arises primarily due to inhomogeneous swelling due to cross-link inhomogeneities, then

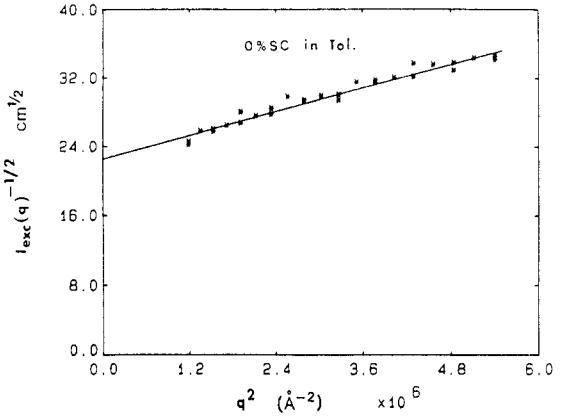

Figure 8. Debye–Bueche plot of light scattering data from PDMS-1000 in toluene.

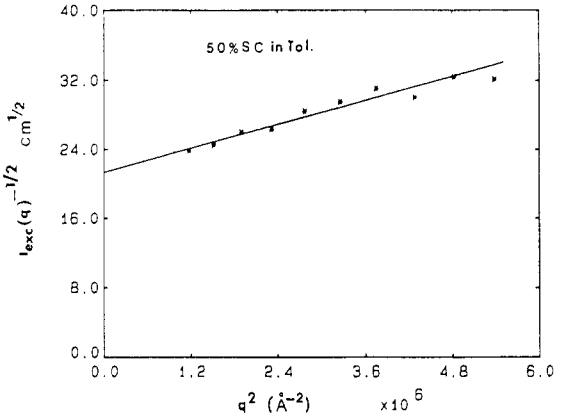

Figure 9. Debye–Bueche plot of light scattering data from PDMS 50% short chains in toluene.

Table V

solvent	mol % short chains	υ_2	a_c,[a] Å	$\langle\eta^2\rangle$[b]	$\langle\eta_0^2\rangle$
toluene	0	0.161	320	19.15×10^{-8}	7.04×10^{-4}
	50	0.251	372	15.24×10^{-8}	14.41×10^{-4}
	90	0.339	364	9.32×10^{-8}	42.85×10^{-4}
	95	0.402	345	9.98×10^{-8}	58.40×10^{-4}
	100	0.504	383	1.01×10^{-8}	18.46×10^{-4}
benzene	0	0.200	380	12.26×10^{-8}	6.09×10^{-4}
	50	0.287	433	13.54×10^{-8}	11.37×10^{-4}
	90	0.380	352	10.12×10^{-8}	30.64×10^{-4}
	95	0.439	356	10.79×10^{-8}	43.96×10^{-4}
	100	0.535	373	0.93×10^{-8}	14.26×10^{-4}

[a] Standard deviation ~10%. [b] Standard deviation ~20%.

according to eq 6

$$R_E(q=0) = \frac{32\pi^3 n^2 \langle\eta^2\rangle a_c^3}{\lambda_0^4} \tag{6a}$$

where $\langle\eta^2\rangle$ is given by eq 21b. Results of the Debye–Bueche plots for the bimodal PDMS networks swollen in toluene and in benzene are given in Table V.

Using eq 6a, we calculated $\langle\eta^2\rangle$ from $R_E(q)$ extrapolated to $q = 0$. However, if $\langle\Delta M_c^2\rangle$ is known, then in principle it should be possible to calculate $\langle\eta^2\rangle$ from eq 21b.

For the case of monodisperse short and long chains, assuming perfect mixing, equal reactivity, and no clustering, the simplest expression for $\langle\Delta M_c^2\rangle$ is

$$\langle\Delta M_c^2\rangle = x(1-x)(M_L - M_S)^2 \tag{32}$$

where x is the mole fraction of short chains. According to eq 32, $\langle\Delta M_c^2\rangle$ would be zero for x equal to zero or one.

Therefore, for a monodisperse unimodal network one would not expect any excess scattering of light. However, this would not be true for a network prepared from a prepolymer having a finite polydispersity.

The Flory–Schulz distribution function[23] can be used to represent the molecular weight distribution of a polydisperse polymer. Let the polydispersity of prepolymer i be

$$[M_w/M_n]_i = 1 + 1/b_i \quad (33)$$

Then for a bimodal network containing short and long chains both of which are polydisperse, the expression for $\langle \Delta M_c^2 \rangle$ is

$$\langle \Delta M_c^2 \rangle = \frac{x M_S^2}{b_S} + \frac{(1-x) M_L^2}{b_L} + x(1-x)(M_L - M_S)^2 \quad (34)$$

The simplest estimate of $\langle \eta^2 \rangle$ due to inhomogeneous cross-linking can be obtained by using eq 34 in eq 21. Such a calculation assumes that the degree of swelling of each chain is determined primarily by the chain length and not by the presence of other chains. This will therefore be considered as a zeroth-order calculation, and the corresponding mean squared fluctuation in scattering power due to cross-link inhomogeneities is represented as $\langle \eta_0^2 \rangle$ in Table V.

In comparing the experimentally measured $\langle \eta^2 \rangle$ with the calculated $\langle \eta_0^2 \rangle$, we note two significant observations:

(i) $\langle \eta_0^2 \rangle$ is much greater than $\langle \eta^2 \rangle$; (ii) in the case of the unimodal networks $\langle \eta^2 \rangle_{x=1} < \langle \eta^2 \rangle_{x=0}$, whereas $\langle \eta_0^2 \rangle_{x=1} > \langle \eta_0^2 \rangle_{x=0}$.

The first observation indicates that the experimentally measured excess scattered intensity is orders of magnitude smaller than that predicted on the basis of a macroscopic theory of swelling of polymer network chains. Light scattering arises due to local fluctuations in the refractive index of the material. The local degree of swelling in the vicinity of a network chain depends not only on the molecular weight of that chain but also on the molecular weights of the chains around it. Therefore, it should be expected that neglect of the presence of neighboring chains in estimating the local fluctuation of concentration or refractive index should result in an overestimate of the excess scattering from inhomogeneously cross-linked networks. The results shown in Table V clearly support such a notion. In order to account for the effect of neighboring chains on the local properties, it is necessary to develop a micromechanical model for the networks.

If one attempts to generalize the Flory–Erman treatment for a bimodal network by assuming that the local degree of swelling depends not on the molecular weight of a particular chain but, rather, on the molecular weight of a cluster of chains in the swelling region, it is apparent that such cluster molecular weights will fluctuate less than will the individual molecular weights, leading in the direction of the observed lowered excess scattering. The larger the cluster, the less will be the fluctuation. This leads to a question regarding the size of the cluster that should be considered. Erman[27] has made the good suggestion that the size is limited by the entanglement molecular weight. Chain entanglements will attenuate the heterogeneity arising from fluctuations in molecular weights between chemical cross-links. If the molecular weight between entanglements is larger than the average molecular weight of the chains spanning the cluster, then the cluster molecular weight will control the local swelling. However, if the cluster is sufficiently large that its span molecular weight is larger than the entanglement molecular weight, then fluctuations in the cluster molecular weight will no longer be significant.

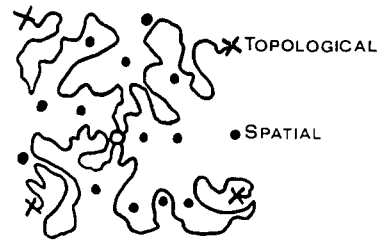

Figure 10. Sketch of topological and spatial neighboring cross-links in a network.

Analytically, it is not easy to account for the effect of the neighboring chains in determining the spatial correlations in swollen networks. Using computer simulation it may be possible to evaluate spatial correlations and thereby estimate the scattered intensity from swollen networks. However, to simulate a real swollen network, there is a need to understand the swelling of network chains at a molecular level.

The small-angle neutron scattering (SANS) experiments by Bastide and Picot[24,25] have revealed that the deformation of a labeled chain between cross-links is much less than that predicted by the affine deformation model. In a perfect tetrafunctional network, there will be four first topological neighboring cross-links for each cross-link point. They are connected to the central cross-link point by a single chain length and are represented by cross marks on Figure 10. In the volume about the central junction point containing the topological neighbors in a dry network there will be other junction points. These junction points are connected to the central junction point by a path through the network that is longer than a single chain length. These are called spatial neighbors of the central junction point and are shown as filled circles in Figure 10. According to Bastide,[24] the swelling of the network is assumed to involve the rearrangement of network chains such that, on changing the macroscopic swelling ratio, the distance between the first topological neighboring cross-links does not change.

The macroscopic swelling behavior of networks is adequately described by the Flory–Erman theory.[8] According to such a theory, the upper and lower limits of the molecular deformation ratio are given by the affine deformation and phantom network models. SANS experiments performed on networks where only the junction points are labeled indicate that the characteristic distances between the labeled points scale reasonably well with the macroscopic swelling ratio.[26] In such an experiment one is observing correlations between spatially neighboring cross-link points, which are closer to each other than the first topological neighboring cross-link points. However, the path through the network that connects two spatially neighboring junction points is expected to be several times longer than a single chain length between topological neighboring cross-links.

On the basis of his SANS results, Bastide[24] has suggested that the network chain unfolding mechanism plays an important role in the swelling of polymer networks. Network unfolding has also been discussed by Ullman.[30] Such a mechanism can qualitatively describe the results for scattering from a network containing labeled paths. However, it is not clear how such a model can be used to describe correlation distances related to spatial fluctuations in the solvent concentrations in a swollen network.

In these light scattering experiments it is observed that the correlation distances, a_c, obtained from the Debye–

Bueche plots, are of the order of 300–400 Å and are relatively independent of the short-chain content. It should be noted that these dimensions are significantly larger than the dimensions of a single chain between cross-links. With the assumption of the phantom network model for deformation, the z-average radii of gyration for single chains in swollen networks consisting of all long (M_n = 22 500) and all short (M_n = 770) chains are estimated to be 74 and 12 Å, respectively. Clearly, the observed correlation distances cover several clusters of topologically neighboring cross-links. It is most likely that at this size scale the solvent concentration fluctuations are related to cross-link heterogeneities due to a distribution of cross-link densities and to network defects such as cyclics and loose ends. For each sample, the detailed network topology and the corresponding solvent concentration fluctuations will depend on the curing conditions.

For our analysis we have assumed that all reactants have equal reactivity at all stages of the cure, leading to a perfect network. However, end-linking leads to imperfections, since reactive chain ends will be stranded, leading to network defects such as cilia. In an attempt to estimate the concentration of defects in bimodal networks, Nomura, Muthukumar, and Stein[28] have resorted to computer simulation of network formation using a lattice model. These two-dimensional calculations suggest that the prevalence of defects greatly increases as long chains are added to a short-chain network, in a manner somewhat similar to our experimental results.

An attempt has been made to test the postulate of equal reactivity of long and short chains by observing small-angle neutron scattering as a function of extent of reaction when deuterium-substituted short chains react with long chains. The preliminary results of these measurements by Wu and co-workers[29] on poly(tetrahydrofuran) networks indicate that short chains react together more rapidly than long ones, leading to a greater degree of clustering and inhomogeneity than for the random model.

IV. Conclusions

These results indicate the difficulty in applying the macroscopic theories of rubber elasticity to describe local swelling characteristics of polymer networks. Light scattering arising due to local refractive index fluctuations is sensitive to the spatial distribution of the solvent. In the case of model networks prepared from randomly mixed prepolymers, the presence of neighboring chains reduces the effect of the bimodal distribution of cross-link density on the local fluctuations in solvent concentration. The discrepancy between the experimental and first-order calculations of $\langle \eta^2 \rangle$ suggests the necessity for an improved treatment for describing the local swelling behavior in real polymer networks.

Acknowledgment. We acknowledge the support of the Center for University of Massachusetts–Industry Research in Polymers (CUMIRP) for these studies as well as the Division of Materials Research of the National Science Foundation and the Materials Research Laboratory of the University of Massachusetts. We appreciate the cooperation of Professor Kenneth Langley of the University of Massachusetts Department of Physics in using his light scattering apparatus along with Dr. Mathew Bishop in offering much helpful advice. We also appreciate discussions with Professors J. E. Mark, K. Dusek, and M. Gottlieb concerning the preparation of the bimodal networks and the interpretation of data. We particularly value the comments of Professors M. Muthukumar and B. Erman in their theoretical interpretation.

Appendix

A. True Scattering Angle. Due to refraction and tilt, the true scattering angle Φ_t in the sample is not the same as the nominal scattering angle θ at which the intensity is measured. For the case of positive (+ve) sample tilt, as shown in Figure 2, the true scattering angle is given by

$$\theta_{true} = \arcsin\{(\sin \Phi_t)/n_r\} + \arcsin\{(\sin(\theta - \Phi_t))/n_r\} \quad \text{(A1)}$$

where n_r is the ratio of the refractive indices of the swollen network to that of the solvent

$$n_r = n_{gel}/n_{solvent}$$

In the following equations Φ_t will represent the magnitude of the tilt angle. Therefore, for –ve tilt

$$\theta_{true} = 180 - \arcsin\{(\sin \Phi_t)/n_r\} - \arcsin\{(\sin(180 - \theta - \Phi_t))/n_r\} \quad \text{(A2)}$$

B. Solid-Angle Correction. The solid angle containing the scattered light flux reaching the detector is different from that in the sample due to refraction. For cylindrical samples, the correction factor was $C_n = n_{sam}^2$ as in eq 28, where n_{sam} is the refractive index of the sample. According to Stein and Keane,[22] for flat, tilted samples (+ve tilt)

$$C_n = \frac{n_{sam}^2}{\cos(\theta - \Phi_t)}\{1 - [(\sin(\theta - \Phi_t))/n_r]^2\}^{1/2} \quad \text{(A3)}$$

C. Scattering Volume Correction. A simple $\sin\theta$ correction is not sufficient. For +ve tilt

$$V_s = \frac{\cos\alpha \cos\phi'}{\cos(\theta - \Phi_t)\sin(\alpha + \phi')\cos\Phi_t} \quad \text{(A4)}$$

where $\phi' = \arcsin[(\sin\Phi_t)/n_r]$ and $\alpha = \arcsin[(\sin[(\theta - \Phi_t))/n_r]$. For –ve tilt

$$V_s = \frac{\cos\beta'' \cos\phi'}{\cos\beta' \sin(\beta'' + \phi')\cos\Phi_t} \quad \text{(A5)}$$

where $\beta' = (180 - \theta - \Phi_t)$ and $\beta'' = \arcsin[(\sin\beta')/n_r]$.

D. Reflection Correction. In the case of flat samples, it is necessary to account for the loss of intensity of the incident and scattered beams due to reflection at the interfaces where there is change in refractive index. The loss of intensity at a particular interface is corrected by dividing the measured intensity by the transmittance, T_i, at that interface

$$Z_i = \frac{1}{T_i} = \frac{1}{1 - r_i} \quad \text{(A6)}$$

where r_i is the reflectance at interface i. The reflectance can be estimated by using the Fresnel equations for reflection.

Let us consider two interfaces A and B. A is the surface of the sample at which the laser beam is incident, and B is the surface from which the scattered beam exits. The incident beam is treated as being vertically polarized and the scattered beam as containing H_v and V_v components. The reflectance of A is given by

$$r_A = \frac{\tan^2(\Phi_t - \phi')}{\tan^2(\Phi_t + \phi')} \quad \text{(A7)}$$

Reflections at B will have two components. For V_v

scattering

$$r_B = \frac{\tan^2 (i - r)}{\tan^2 (i + r)} \tag{A8}$$

and for H_v scattering

$$r_B = \frac{\sin^2 (i - r)}{\sin^2 (i + r)} \tag{A9}$$

In equations A8 and A9, we have for (i) +ve tilt, $i = \alpha$ and $r = (\theta - \Phi_t)$; and for (ii) -ve tilt, $i = \beta''$ and $r = \beta'$. Therefore, for a particular scattering geometry, the total reflection correction is

$$Z = \frac{1}{(1 - r_A)(1 - r_B)} \tag{A10}$$

References and Notes

(1) Stein, R. S. *J. Polym. Sci., Polym. Lett. Ed.* **1969**, *7*, 657.
(2) Bueche, F. *J. Colloid Interface Sci.* **1970**, *33*, 61.
(3) Debye, P.; Bueche, A. M. *J. Appl. Phys.* **1949**, *20*, 518; Debye, P.; Anderson, H. R.; Brumberger, H. *J. Appl. Phys.* **1957**, *28*, 679.
(4) Treloar, L. R. G. *The Physics of Rubber Elasticity*; Clarendon: Oxford, 1975.
(5) Mark, J. E.; Sullivan, J. L. *J. Chem. Phys.* **1977**, *66*, 1006.
(6) Mark, J. E. *Adv. Polym. Sci.* **1982**, *44*, 1.
(7) Llorente, M. A.; Mark, J. E. *J. Chem. Phys.* **1979**, *71*, 682.
(8) Flory, P. J.; Erman, B. *Macromolecules* **1982**, *15*, 800, 806.
(9) Mark, J. E. *Elastomers and Rubber Elasticity*; Mark, J. E., Lal, J., Eds.; American Chemical Society: Washington, DC, 1982.
(10) Kerker, M. *The Scattering of Light*; Academic Press: New York, 1969.
(11) Einstein, A. *Ann. Phys.* **1910**, *33*, 1275.
(12) Bullough, R. K. *J. Polym. Sci.* **1960**, *46*, 517.
(13) Huglin, M. B.; Sokro, M. B. *Polymer* **1980**, *21*, 651.
(14) Flory, P. J. *Principles of Polymer Chemistry*; Cornell University Press: Ithaca, NY, 1953.
(15) Debye, P.; Bueche, A. M. *J. Chem. Phys.* **1950**, *18*, 1423.
(16) Flory, P. J.; Rehner, J., Jr. *J. Chem. Phys.* **1943**, *11*, 521.
(17) Wun, K. L.; Prins, W. *J. Polym. Sci., Polym. Phys. Ed.* **1974**, *12*, 533.
(18) Soni, V. K. Ph.D. Dissertation, University of Massachusetts, Amherst, 1986.
(19) Meyers, K. O.; Bye, M. L.; Merrill, E. W. *Macromolecules* **1980**, *13*, 1045.
(20) Kaye, W.; McDaniel, J. B. *Appl. Opt.* **1974**, *13*, 1934.
(21) Johnson, B. L.; Smith, J. *Light Scattering from Polymer Solutions*; Huglin, M. B., Ed.; Academic Press: New York, 1972.
(22) Stein, R. S.; Keane, J. J. *J. Polym. Sci.* **1955**, *17*, 21.
(23) Schulz, G. V. *Z. Phys. Chem.* **1939**, *B43*, 25.
(24) Bastide, J.; Picot, C.; Candau, S. *J. Macromol. Sci., Phys.* **1981**, *B19*, 13.
(25) Candau, S.; Bastide, J.; Delsanti, M. *Adv. Polym. Sci.* **1982**, *44*, 27.
(26) Benoit, H., et al. *J. Polym. Sci., Polym. Phys. Ed.* **1976**, *14*, 2119.
(27) Erman, B., private communication.
(28) Nomura S.; Muthukumar, M.; Stein, R. S., manuscript in preparation.
(29) Wu, W. L.; Jong, L.; Hanyu, A.; Stein, R. S., submitted for publication.
(30) Ullman, R. *Macromolecules* **1982**, *15*, 582.